VERTICAL DISPERSION BUMP DESIGN FOR FEMTO-SECOND SLICING BEAMLINE AT THE ALS*

C. Sun†, C. Steier and W. Wan,
Lawrence Berkeley National Laboratory, Berkeley, CA 94720, USA

Abstract

Femto-second (fs) slicing beamline has been brought to the operation at the Advanced Light Source (ALS) since 2002. It employs the resonant interaction of an electron bunch with a fs laser beam in a wiggler to energy-modulate a short section of the bunch. The induced energy modulation is then converted to a transverse displacement using a vertical dispersion bump downstream of the wiggler. Thus, the radiation from the fs pulse can be separated from the main bunch radiation. The current dispersion bump design has proved to be an effective and reliable one. However, the ALS storage ring lattice is under an upgrade to improve its brightness. After the completion of the upgrade, a new low emittance lattice will be implemented, and the current dispersion bump design needs to be modified to provide the adequate vertical displacement, while minimizing the vertical emittance and spurious dispersion. In this paper, we present the new design of a vertical dispersion bump using Multi-Objective Genetic Algorithm (MOGA) for the ALS upgrade lattice.

INTRODUCTION

The Advanced Light Source (ALS) is one of the earliest third generation synchrotron light sources at Lawrence Berkeley National Laboratory and is serving more than 2200 users every year. To generate short pulses of x-rays with duration of few-hundred femtoseconds, an innovative technique to slice longer electron bunches has been proposed [1] and successfully demonstrated 10 years ago [2] at the ALS. It employs the resonant interaction of an electron bunch with a femtosecond (fs) laser beam in a modulator (such as a wiggler) to energy-modulate a short section of the bunch. The induced energy modulation is then converted to a transverse displacement using a vertical dispersion bump downstream of the modulator. When the electron bunch go through the radiator (such as an undulator or a bending magnet), the radiation from the fs-sliced electron bunch can be separated from the main bunch radiation. With apertures in the beamline to block the radiation for the unsliced part of the bunch, we can then produce fs x-ray pulse. The schematic of a fs slicing beamline is shown in Fig. 1.

Initially, a bending magnet has been used as a radiator for scientific experiments until 2005 [2, 3]. Based on the performance limitations of this bending magnet beamline,

* Work supported by the United States Department of Energy under Contract No. DE-AC02-05CH11231.

† CCSun@lbl.gov

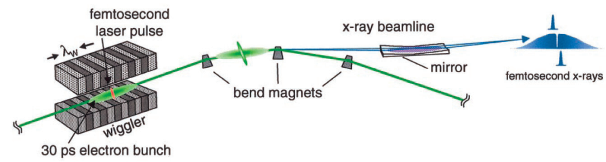

Figure 1: Schematic of a femtosecond slicing beamline [2].

particularly the very low flux, an upgrade to an undulator beamline was successfully implemented in 2007 [4, 5], which enables more experiments that make use of time resolved spectroscopic techniques and require higher average photon flux. The dispersion bump has proved to be an effective and reliable design to separate the fs sliced bunch from the main bunch. To keep the ALS competitive with new synchrotron light sources, however, the ALS storage ring lattice is under an upgrade to improve its brightness [6]. After the completion of the upgrade, a new low emittance lattice will be implemented, and the current dispersion bump design need to be modified to provide the adequate vertical displacement, while minimizing the vertical emittance and spurious dispersion. In this paper, we present the new design of a vertical dispersion bump using Multi-Objective Genetic Algorithm (MOGA) for the ALS upgrade lattice [7]. First, we briefly introduce matrix notations of global and local couplings of a linear lattice.

GLOBAL AND LOCAL COUPLING

The 4×4 one-turn transfer matrix $\mathbf{T}$ of a storage ring can be written as

$$\mathbf{T} = \begin{pmatrix} \mathbf{M} & \mathbf{m} \\ \mathbf{n} & \mathbf{N} \end{pmatrix}, \tag{1}$$

where $\mathbf{M}, \mathbf{N}, \mathbf{m}$ and $\mathbf{n}$ are 2×2 matrices. For an uncoupled lattice, the matrices $\mathbf{m}$ and $\mathbf{n}$ equal zero, and the transfer matrix $\mathbf{T}$ is block diagonal. In the presence of coupling, however, we can decompose the matrix $\mathbf{T}$ into a normal mode as [8, 9, 10]

$$\mathbf{T} = \mathbf{V}\mathbf{U}\mathbf{V}^{-1}, \tag{2}$$

where the normal mode matrix $\mathbf{U}$ is block diagonal and the coupling matrix $\mathbf{V}$ is symplectic. They are given by [8, 9, 10]

$$\mathbf{U} = \begin{pmatrix} \mathbf{A} & \mathbf{0} \\ \mathbf{0} & \mathbf{B} \end{pmatrix}, \mathbf{V} = \begin{pmatrix} \gamma\mathbf{I} & \mathbf{C} \\ -\mathbf{C}^{\dagger} & \gamma\mathbf{I} \end{pmatrix}, \tag{3}$$

where $\mathbf{I}$ is the identity matrix, "†" is the symplectic conjugator, and $\gamma^2 + ||\mathbf{C}|| = 1$.

The block diagonal matrix $\mathbf{U}$ defines two uncoupled eigenmode motions. The two eigentunes are given by

$$\cos 2\pi\nu_{a,b} = \frac{1}{4}Tr[\mathbf{M}+\mathbf{N}] \pm \frac{1}{4}\sqrt{Tr[\mathbf{M}-\mathbf{N}])^2 + 4||H||}, \tag{4}$$

where

$$\mathbf{H} \equiv \mathbf{m} + \mathbf{n}^+. \tag{5}$$

Therefore, the tune separation of the two normal modes is given by

$$(\cos 2\pi\nu_a - \cos 2\pi\nu_b)^2 = \frac{1}{4}(Tr[\mathbf{M}-\mathbf{N}])^2 + ||H||. \tag{6}$$

On the coupling resonance, $Tr[\mathbf{M}-\mathbf{N}] = 0$, the minimal separation $\delta\nu = \sqrt{||\mathbf{H}||}/(2\pi \sin 2\pi\nu)$. The closet approach of tune ν_a and ν_b is one measure of the global coupling in the lattice. The procedure to minimize $\delta\nu$ is often called global decoupling.

The matrix $\mathbf{C}$ characterize the amount of local coupling in a lattice. If $\mathbf{C} = 0$, then $\mathbf{V} = 1$ and the motion is decoupled. However, it is convenient to normalize out the Twiss function dependence in $\mathbf{C}$ via the matrix $\mathbf{G}$

$$\mathbf{G} = \begin{pmatrix} \mathbf{G}_a & \mathbf{0} \\ \mathbf{0} & \mathbf{G_b} \end{pmatrix}, \tag{7}$$

where

$$\mathbf{G_{a,b}} = \begin{pmatrix} \frac{1}{\sqrt{\beta_{a,b}}} & \mathbf{0} \\ \frac{\alpha_{a,b}}{\beta_{a,b}} & \sqrt{\beta_{a,b}} \end{pmatrix}. \tag{8}$$

Thus, the normalized normal mode matrix $\overline{\mathbf{U}}$ and coupling matrix $\overline{\mathbf{V}}$ are given by

$$\overline{\mathbf{U}} = \mathbf{G}\mathbf{U}\mathbf{G}^{-1}, \overline{\mathbf{V}} = \mathbf{G}\mathbf{V}\mathbf{G}^{-1} = \begin{pmatrix} \gamma\mathbf{I} & \overline{\mathbf{C}} \\ -\overline{\mathbf{C}}^+ & \gamma\mathbf{I} \end{pmatrix}, \tag{9}$$

and

$$\overline{\mathbf{C}} = \mathbf{G}_a\mathbf{C}\mathbf{G}_b^{-1}. \tag{10}$$

$\overline{\mathbf{C}}$ is useful for characterizing the local coupling. The rms beam size in the x and y planes for the a mode are [11]

$$\sigma_{x,a} = \gamma\sqrt{\epsilon_a\beta_a}, \quad \sigma_{y,a} = \sqrt{\epsilon_a\beta_b}\sqrt{\overline{C}_{22}^2 + \overline{C}_{12}^2}, \tag{11}$$

where ϵ_a is the a mode emittance, β_a is the beta function of a mode. The local coupling for the a mode is given by

$$\mathbf{R}_a = \frac{\sigma_{y,a}}{\sigma_{x,a}} = \frac{1}{\gamma}\sqrt{\frac{\beta_b}{\beta_a}}\sqrt{\overline{C}_{22}^2 + \overline{C}_{12}^2}. \tag{12}$$

For b mode, the rms beam size are

$$\sigma_{x,b} = \sqrt{\epsilon_b\beta_a}\sqrt{\overline{C}_{11}^2 + \overline{C}_{12}^2}, \quad \sigma_{x,b} = \gamma\sqrt{\epsilon_b\beta_b}, \tag{13}$$

and the coupling is

$$\mathbf{R}_b = \frac{\sigma_{x,b}}{\sigma_{y,b}} = \frac{1}{\gamma}\sqrt{\frac{\beta_a}{\beta_b}}\sqrt{\overline{C}_{11}^2 + \overline{C}_{12}^2}. \tag{14}$$

Thus, to reduce the local coupling, we can minimize the coupling ratio $\mathbf{R}_{a,b}$ of both normal modes.

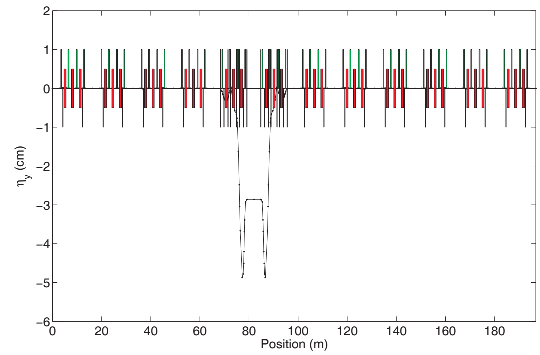

Figure 2: Vertical Dispersion Bump.

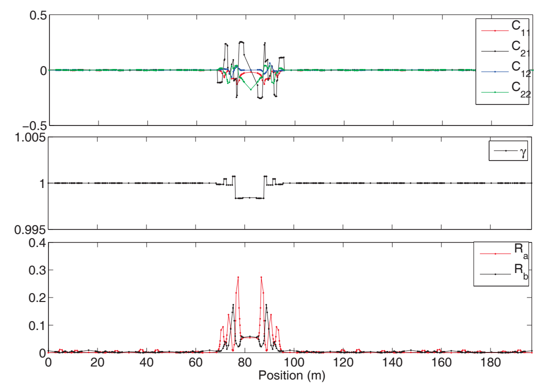

Figure 3: Local coupling at different locations. (Top) coupling matrix $\mathbf{C}$ element, (Middle) coupling coefficient γ and (Bottom) coupling ratio $\mathbf{R}_a$ and $\mathbf{R}_a$.

DISPERSION BUMP DESIGN

To separate the sliced bunch from the main bunch, different techniques can be used. The vertical dispersion bump design is used at the ALS since it allows the use of the radiator in wiggler mode and the use of dispersive spectroscopy in the beamline. The dispersion bump is created using skew quadrupole by coupling the horizontal dispersion into the vertical plane. The design was demonstrated using only 4 skew quadrupoles at the ALS in 2002 [3]. This was the minimum scheme to generate a closed dispersion bump because coincidentally the phase advance between the skew quadrupoles cancel coupling effects nearly perfectly. However, while the beamline was being built, a new improved lattice was implemented in the ALS. It features smaller beta functions in straights resulting in higher brightness. However, the phase advance between the skew quadrupoles for the dispersion bump in the new lattice changed enough that the cancellation effect with respect to coupling did not work any more. Therefore, a modification of the skew quadrupole scheme was required: 12 (instead of 4) skew quadrupoles are used, spanning 3 (instead of 2) arcs [5]. Although this design is complex, it has proved to be an effective one and is used in the routine operation.

To keep the ALS competitive in the frontier of soft x-ray

ISBN 978-3-95450-115-1

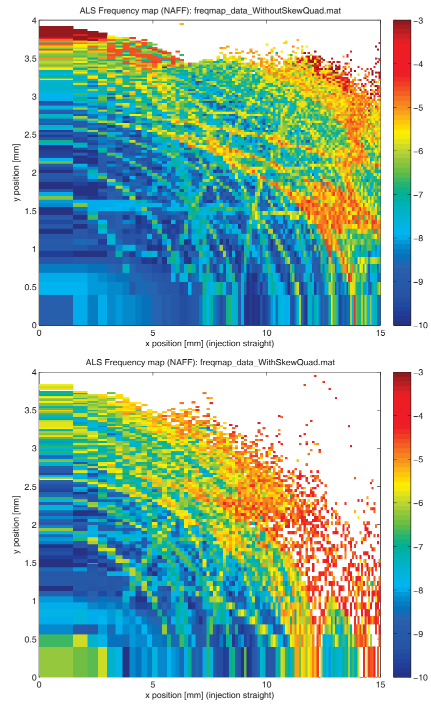

Figure 4: Dynamic aperture with (top) skew quads off and (bottom) skew quads on.

synchrotron radiation sources, the ALS storage ring lattice is under an upgrade to improve its brightness [6]. After the completion of the upgrade, total 48 (four families) combined sextupole/corrector/skew-quadrupole multi-magnets will be installed and a new low emittance lattice will be implemented. The current dispersion bump design needs to be revisited to provide the adequate vertical displacement, while minimizing the vertical emittance and spurious dispersion. Since additional four families skew quadrupoles are installed, we have more knobs to create the dispersion bump. The new scheme will have 12 skew quads, symmetrically spanning 2 arcs. To minimize the vertical emittance and spurious dispersion, for the bump design we need to minimize the global coupling $||\mathbf{H}||$, the local coupling everywhere ($\mathbf{R}_a$ and $\mathbf{R}_b$), and the dispersion outside of the bump, and maximize the dispersion inside the bump (straight 6). It is a multi-objective and multi-variable optimization problem. The Multi-Objective Genetic Algorithm [7] (MOGA) is applied for this design. One of the bump solution is shown in Fig. 2. It has 4 cm amplitude bump, and the dispersion function is close to zero outside of the bump. Fig. 3 shows the local couplings which are minimized along the ring.

The main issue that has been studied in connection with the vertical dispersion bump design is its impact on the nonlinear dynamics of the ALS storage ring, particularly dynamic aperture and lifetime. The Figs. 4 and 5 show the dynamic aperture and Touschek lifetime comparison before skew quadrupoles turn on and off. Clearly, the dispersion bump does not have an significant impact on them.

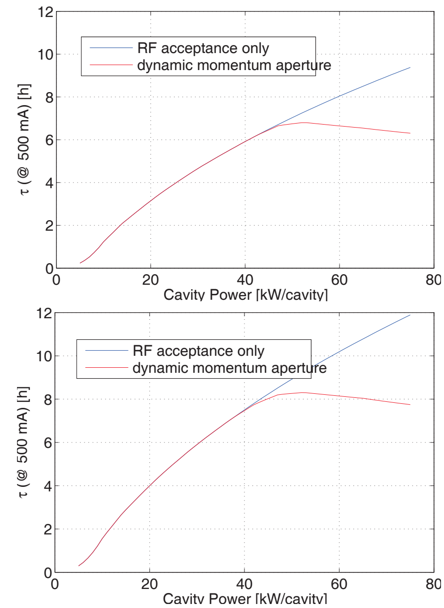

Figure 5: Touschek lifetime with (top) skew quads off and (b) skew quads on.

CONCLUSIONS

Using MOGA, we have successfully designed a vertical dispersion bump for the fs slicing beamline at the ALS, and evaluated its impact on the nonlinear dynamics of the storage ring. This design could provide a sufficient dispersion bump to separate the fs sliced pulse from the main bunch radiation, while minimizing its impacts on the nonlinear beam dynamics of the storage ring as well as other beamlines.

REFERENCES

[1] A. A. Zholents and M. S. Zolotorev, Phys. Rev. Lett. 76, 912915 (1996).

[2] R. W. Schoenlein *et al.*, Science **287**, 2237(2000).

[3] C. Steier *et al.*, in *Procceedings of the Particle Accelerator Conference, 2003* (IEEE, Portland, OR, 2003), p.397.

[4] C. Steier *et al.*, in *Procceedings of the Particle Accelerator Conference, 2005* (IEEE, Knoxville, TN, 2005), p.4096.

[5] C. Steier *et al.*, in *Procceedings of the Particle Accelerator Conference, 2007* (IEEE, Albuquerque, NM, 2007), p.1194.

[6] C. Steier *et al.*, Nucl. Instr. and Meth. A 649, (2011) 2529.

[7] K. Deb, IEEE transactions on evolutionary computation, vol. 6, no. 2, 2002, pp.192-197.

[8] D. A. Edward and L. C. Teng, IEEE Transactions on Nuclear Science, June 1973, Volume NS-20, Number 3, p.885.

[9] S. Peggs, IEEE Transctions on Nuclear Science, Agust 1983, Volume NS-30, Number 4, p.2460.

[10] P. Bagley and D. Rubin, in *Proceedings of the Particle Accelerator Conference, Chicago, Illinois* (IEEE, Piscataway, NJ, 1989), p.874.

[11] D. Sagan and D. Rubin, Phys. Rev. ST Accel. Beams 2, 074001 (1999).